Soil & Tillage Research 222 (2022) 105418

Contents lists available at ScienceDirect

Soil & Tillage Research

journal homepage: www.elsevier.com/locate/still

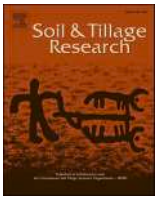

A high-resolution physical modelling approach to assess runoff and soil erosion in vineyards under different soil managements

Eugenio Straffelini [a,*], Anton Pijl [a], Stefan Otto [b], Enrico Marchesini [c], Andrea Pitacco [d], Paolo Tarolli [a]

[a] Department of Land, Environment, Agriculture and Forestry, University of Padova, Agripolis, Viale dell'Università 16, Legnaro (PD) 35020, Italy
[b] National Research Council, Institute for Sustainable Plant Protection (IPSP), Agripolis, Viale dell'Università 16, Legnaro (PD) 35020, Italy
[c] Agrea s.r.l, Via Garibaldi 5, San Giovanni Lupatoto (VR) 37057, Italy
[d] Department of Agronomy, Food, Natural Resources, Animals and Environment, University of Padova, Agripolis, Viale dell'Università 16, Legnaro (PD) 35020, Italy

ARTICLE INFO

Keywords:
Vineyard
Soil management
Runoff
Soil erosion
Modelling
UAV-SfM

ABSTRACT

Steep-slope viticulture is a common practice in the Mediterranean basin, and provides landscapes of considerable socio-economic value. However, these complex agricultural systems are intrinsically fragile. One of the main problems is soil erosion due to extreme rainfall events. This may cause a progressive reduction in soil fertility and the occurrence of instabilities and land degradation phenomena. To worsen this condition there is the increasing mechanisation of agricultural management causing soil compaction, and the pressure of climate change, with an intensification of extreme weather events. In this context, vineyard soil management plays a key role, as it can accelerate or mitigate overland flow and soil erosion phenomena. There are various techniques for quantifying these processes, often based on field measurements through prolonged data collection using experimental plots. However, the advent of new technologies in remote sensing opens new frontiers in the acquisition of high-resolution spatial data. Indeed, they could be used in runoff/erosion simulation models and integrated with site-specific data.

The aim of this paper is to assess runoff and soil erosion processes in vineyard under four different soil managements. Specifically, four practices were tested: (1) Reference (inter-row managed with standard farm grass cover; RF); (2) Continuous Tillage (bare soil obtained by continuous mechanical weeding using roto-tiller; CT); Nectariferous (a mix of herbaceous species capable of attracting insects favouring inter-row biodiversity; NF); (4) Single Tillage (inter-row weeding once a year using roto-tiller; ST). The research proposes a modelling approach using a physically-based model (SIMWE) using samples of runoff and sediment as an assessment, collected with a low-cost methodology. In particular, a cost-effective approach easily replicable in different contexts (such as developing countries) is sought. In addition to cultivation specifics, areas of soil compacted by the passage of agricultural vehicles were also analysed using the connectivity index. In general, results show an interesting capacity of ST in mitigating soil erosion, as well as for NF. Furthermore, the negative role of wheel tracks as preferential pathways for surface runoff and sediment is highlighted. Finally, the work shows that CT aggravated soil erosion as compared to RF.

Abbreviations: AWC, Available Water Capacity; ANOVA, Analysis of Variance; CI, Index of Connectivity; CP, Check Points; CT, Continuous Tillage; DEM, Digital Elevation Model; DoD, DEM of Difference; FAO, Food and Agriculture Organization; GCP, Ground Control Point; GIAHS, Globally Important Agricultural Heritage Systems; GNSS, Global Navigation Satellite System; HRT, High-Resolution Topography; KINEROS, Kinematic Runoff and Erosion Model; LiDAR, Laser Detection and Ranging; MAE, Mean Absolute Error; ME, Mean Error; MSV, Multi-Stereo-View; NF, Nectariferous; NMAD, Normalised Median Absolute Deviation; PDF, Probability Density Function; RE, Rainfall Event; RF, Reference; RMSE, Root Mean Squared Error; RTK, Real-Time Kinematic; RUSLE, Revised Universal Soil Loss Equation; SDE, Standard Deviation; SfM, Structure-from-Motion; SIMWE, Simulation Water Erosion; ST, Single tillage; UAV, Uncrewed aerial vehicle; UNESCO, United Nations Educational, Scientific and Cultural Organization; VI, Vine Rows; WEPP, Watershed Erosion Prediction Project; WT, Wheel Tracks.

* Correspondence to: Padova, Agripolis, Viale dell'Università 16, 35020 Legnaro, PD, Italy.
E-mail address: eugenio.straffelini@unipd.it (E. Straffelini).

https://doi.org/10.1016/j.still.2022.105418
Received 19 July 2021; Received in revised form 5 April 2022; Accepted 22 April 2022
Available online 17 May 2022

1. Introduction

Hilly and mountainous viticulture offers important economic, social and landscape value for the territories in which it is practised. Indeed, several international programmes recognise the importance of these landscapes by including them in lists aimed at their protection and promotion. For example, the FAO launched the GIAHS (*Globally Important Agricultural Heritage Systems*) programme, including the Soave wine-growing area (northern Italy) devoted to heroic viticulture following traditional practices (FAO, 2021). Also, UNESCO has recognised the cultural heritage of steep-slope wine-growing landscapes, such as the Prosecco production zone in Italy (UNESCO, 2021).

Hillsides are morphologically suitable for vine cultivation for several reasons, mainly related to climate conditions. Frosts in late spring could severely damage the production (Di Giuseppe et al., 2020), while high temperatures during the growing season could affect the photosynthesis of the vine due to stomatal closure (Greer and Weedon, 2012). Proper exposure to sunlight provided by an inclined terrain can mitigate the impact of these phenomena (Townsend, 2011). Indeed, a vineyard placed on a slope receives more insolation than a flat one, increasing the growing degree-days, and enables cold air to drain away (Jones and Hellman, 2003). On the other hand, such landscapes are more affected by processes occurring on the Earth surface, mainly those related to the water cycle and soil erosion. This is a major concern in the perspective of climate change, which will significantly affect steep-slope agriculture globally (Wang et al., 2022). In the Mediterranean basin, soil erosion is a serious threat due to high rainfall intensity and the complex geomorphology where vineyards are widespread (Poesen and Hooke, 1997; Rodrigo Comino et al., 2016). These factors can trigger land degradation (Lal, 2001), slope failures and collapses in agricultural fields (Jing et al., 2019), as well as lead to soil fertility reduction (Novara et al., 2018).

Research solutions to mitigate soil erosion in steep vineyards is a priority to ensure sustainable production. In this challenge, the land manager plays a central role in soil loss generation and his choices could make a substantial difference. A widely used approach to protect the soil from erosion is the implementation of grass covers. Several authors reported on the potentials of vegetation cover in mitigating erosion (Monteiro and Lopes, 2007; Marques et al., 2010; Ruiz-Colmenero et al., 2011). It offers direct surface protection from the kinetic force of the raindrop, which can erode soil particles through the splash effect. Furthermore, thanks to the complex root network, it positively influences the water balance in the soil, as well as the structural stability (Vergani and Graf, 2016). In addition, vines can benefit from soil richer in organic matter, which stabilises the macro-aggregates and limits the formation of crusts (Angulo-Jaramillo et al., 2016). On the contrary, tillage operation could accelerate soil erosion in steep-slope vineyards. While it may provide benefits, such as weed control and a temporary increase in soil water infiltration (Buesa et al., 2021), the increased rate of soil loss cannot be neglected. For instance, in a study conducted in Italy, it was observed that the sediment yield in a tilled plot was 9 times higher than in a grass cover plot (Biddoccu et al., 2017). The research also pointed out the role of mechanisation in favouring runoff generation and erosion processes. To understand the influence of this factor, it is possible to refer to a work conducted by Pijl et al. (2019), where a 37% increase in potential soil erosion in mechanised fields compared to non-mechanised fields was estimated. This could be attributed to soil compaction, a process that alters the physical characteristics of the soil, reducing its permeability and increasing runoff and erosion (Batey, 2009). The vineyard configuration on steep slopes, as well as vine rows layout, can also have consequences on the soil surface processes (Tarolli and Straffelini, 2020). The development of agricultural machinery is leading modern viticulture to adopt slope-wise cultivation systems (Corti et al., 2011). However, this vineyard design evolution has serious impacts on surface runoff and soil erosion, a fact also recently observed and quantified by Pijl et al. (2022). The authors illustrate that cultivation along the slope designed for agricultural machinery tends to produce surface runoff with considerable sediment concentration rates.

Quantifying these processes in steep-slope agriculture is important to provide stakeholders with guidelines for sustainable management. Various methods are available in the literature for this purpose. For example, some authors propose the use of experimental plots in vineyards for measuring the sediment transported after precipitation (Novara et al., 2011; Biddoccu et al., 2016). In this framework, remote sensing is an interesting tool to understand the problem. The advent of 3D surveying technologies and the implementation of innovative data management methods open up new opportunities (Tarolli and Straffelini, 2020). For example, LiDAR allows the reconstruction of agricultural land at different spatial scales using different platforms, from plot-level up to larger scales (Ladefoged et al., 2011; Barneveld et al., 2013). Nowadays, a rapid and low-cost solution is the Structure-from-Motion (SfM) technique paired with the Multi-Stereo-View (MSV) algorithm and using a drone (UAV-SfM). This High-Resolution Topography (HRT) procedure allows the construction of Digital Elevation Models (DEMs), permitting the digitalisation of even the smallest surface signatures (Oz et al., 2017). They could be used in surface processes investigations (Carrivick et al., 2016), offering interesting outcomes in erosion analysis (Pineux et al., 2017; Meinen and Robinson, 2020). A remotely sensed method for the quantification of soil losses is the use of multiple DEMs from repeated surveying to highlight eroded areas and sedimentation spots (DEMs of Difference - DoD; Martínez-Casasnovas et al., 2002; Arriola-Valverde et al., 2020; Cândido et al., 2020). This is a purely morphological approach that highlights the geometric differences between surfaces, but does not address the causal processes, such as rain erosivity or runoff generation. An alternative that may overcome these limitations is numerical models for erosion quantification, which require georeferenced input data (Boardman and Favis-Mortlock, 1998). The Revised Universal Soil Loss Equation (RUSLE) is a widely-used example of a model to predict average annual soil loss by water implementing diverse factors (rainfall erosivity, soil erodibility, topography, cover and practice management; Renard et al., 1991). However, as an empirical and simplified equation, the model has some limitations (Tang et al., 2015; Alewell et al., 2019). To refine the quantification of the erosion process, physically-based models have been developed (Nearing et al., 1994). For instance, the Watershed Erosion Prediction Project (WEPP) models requires climatic, soil, topographic and management inputs to provide outputs of water balance, soil detachment, transportation and deposition (Laflen et al., 1991). The Kinematic Runoff and Erosion Model (KINEROS) runoff and erosion model describes the processes of interception, infiltration, surface runoff and erosion in agricultural and urban watersheds (Smith et al., 1995). The Simulation Water Erosion (SIMWE) is a landscape-scale simulation model of overland flow, soil erosion, sediment transport and deposition designed for spatially variable terrain, soil, cover and rainfall excess conditions (Mitasova et al., 2004). However, physically-based models are often complex and require considerable input data (e.g. soil properties, hydrology, topography, vegetation) with high spatial and temporal resolution, resulting in costly and difficult implementation (Arriola-Valverde et al., 2020). The use of digital models from UAV-SfM as input in modelling may provide fast access to high-resolution data. In addition, they can help to understand how the vineyard system is connected in terms of runoff and soil particles with the downstream area. Connectivity indices are tools for understanding the pathways that govern the delivery of sediment from the hillslope (Cucchiaro et al., 2019). Traditionally, they are used to understand the processes taking place at catchment level, and how they are connected to the hydrographic network, but they also have applications in agriculture (Heckmann et al., 2018).

In this paper, we propose a modelling approach for the analysis of overland flow and soil erosion in steep-slope vineyards, to evaluate different types of inter-row soil management (Reference Tillage, Continuous Tillage, Nectariferous and Single Tillage). The SIMWE model is used for the simulation of runoff following rainfall of varying intensity, as well as the concentration of eroded sediment transported by

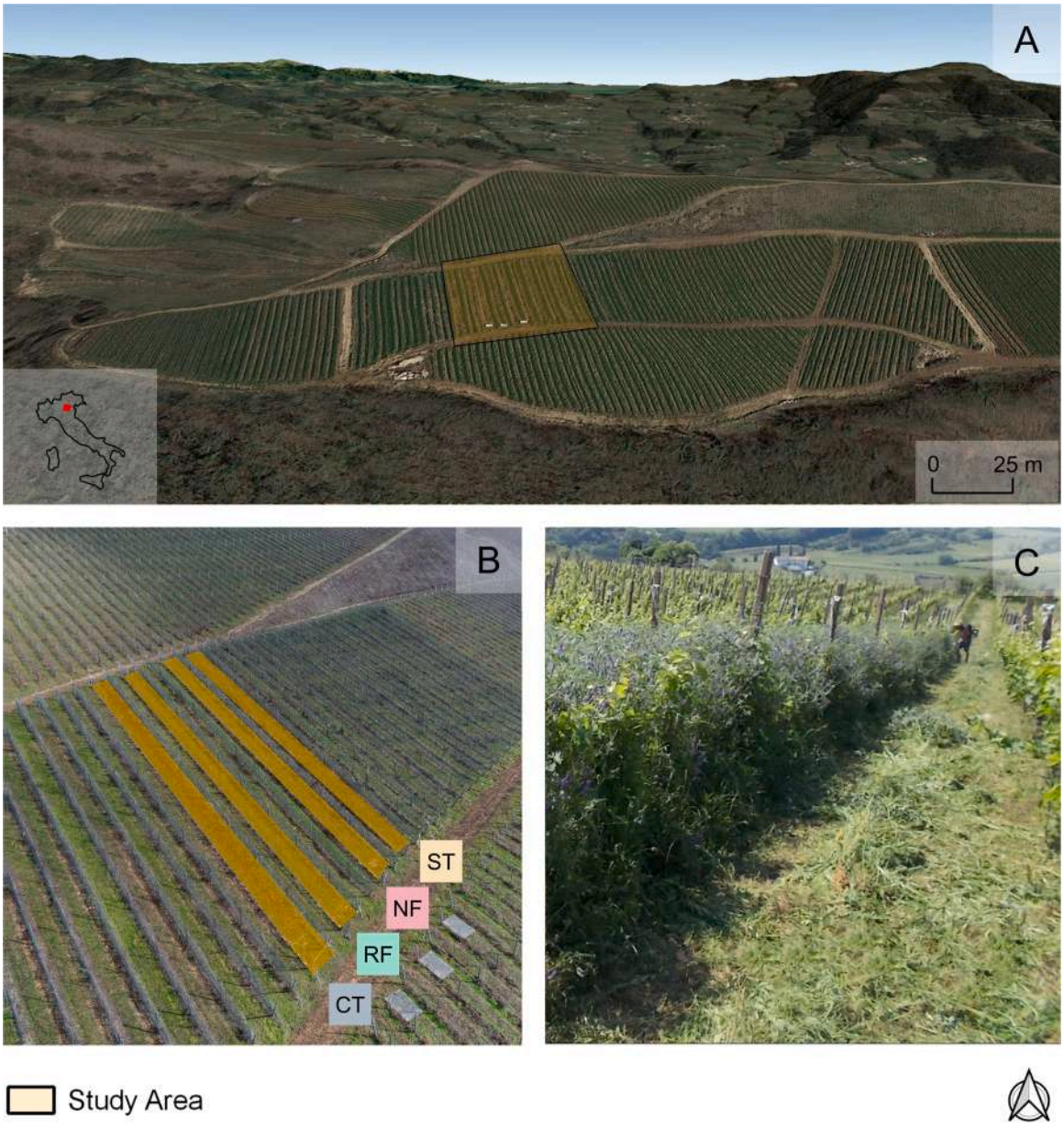

Fig. 1. Situation of the study area, showing a typical steep vineyard slope found in northern Italy (A; 3D landscape provided by Google®), with the four practices of continuous tillage CT, reference RF, nectariferous cover NF, and single tillage ST placed in parallel inter-rows (B; aerial photo by S. Cucchiaro) of homogeneous length and slope (C; photo by S. Otto).

water. It is based on a high-resolution DEM of the study area, meteorological records, in-field measurements (such as soil infiltration rate) and literature parameters. In addition, the application of a sediment and flow index of connectivity is proposed as a useful approach to understand and map the preferential runoff and sediment paths along the inter-row to downstream, thus identifying possible typical patterns for specific cultivation practices. The application of this index provides an insight into the impacts of heavy mechanisation in vineyards, which alters sediment transport processes through tyre tracks. Finally, the modelled results are assessed by experimental plot monitoring over a year, where water and sediment were collected using low-cost methods. Therefore, the final objective is to evaluate which management is most effective in limiting runoff and soil erosion generation in steep viticulture, to offer guidance to stakeholders for better management.

2. Material and methods

2.1. Study area

The experimental vineyard where the research was carried out is located on a hill in northern Italy, in the Veneto region (45°30'29.93" N; 11°12'53.17" E; 565 m a.s.l.; Fig. 1A, B, C). The landscape is characterised by rounded hillsides historically cultivated with vines. It is part of the Globally Important Agricultural Heritage Systems (GIAHS) site called "*Soave Traditional Vineyards*", a cultural landscape where viticulture began to spread as early as Roman times (FAO, 2020). The vineyard under study is arranged along slope lines (in Italian "*ritto-chino*") and is managed using agricultural machinery. According to the regional soil map (ARPAV, 2019), the area is characterised by a marly lime substrate that mainly consists of fine clay granulometry. A soil pit revealed a fairly deep profile (roughly 1.8 m) above a coarse gravel layer (about 1.5 m down to the bedrock), while sample analysis showed a

Table 1
Species composition of nectariferous mix planted in the NF inter-row practice.

Species	Common name	Family	% in the mix (mass-based)	Kg ha^{-1}
Avena sativa L.	Oat	Gramineae	25	37
Vicia villosa Roth	Vetch	Leguminosae	20	30
Trifolium incarnatum L.	Scarlet clover	Leguminosae	6	9
Vicia faba L.	Faba bean	Leguminosae	35	53
Fagopyrum esculentum	Buckwheat	Polygonaceae	10	15
Phacelia tanacetifolia Benth.	Phacelia	Boraginaceae	4	6

texture consisting of 43.3% clay, 18.3% silt and 38.4% sand. The soil is characterised by a high stoniness (up to 50%), clearly observable also after tillage operations. All these information guided the authors in the further selection of model input parameters (see Section 2.4).

2.2. Inter-row experimental design

The research was carried out in four inter-rows of an experimental vineyard separated from each other by a buffer inter-row. This allowed analysing runoff and erosion phenomena separately for each type of management, permitting a final comparison. Each inter-row has a length of 42 m and a width of 2 m and is hydrologically isolated. Indeed, an agricultural road is located upstream intercepting the runoff and driving it to a drainage system located outside the study area. The vineyard is located on a morphologically uniform and mechanically levelled slope with an average slope of 27.9%. The hydrological conditions of the site, as well as the uniform slope, were decisive in the choice of the site. In this way, error in the comparison of results due to possible non-uniformity between the study areas is minimised. Four types of management were tested:

(1) Reference (RF), an inter-row where the farm's standard grass cover management is used. Specifically, the inter-row is covered by grass and cover crops (mostly *Medicago sativa*, also including *Trifolium repens, Taraxacum officinale, Geranium molle, Rumex crispus, Lolium sp.*) that are typically used in this vineyard. Agricultural machinery was used for the standard annual management of the vineyard, consisting of 3–5 grass mowings per year.
(2) Continuous tillage (CT). Inter-row with continuous mechanical weeding, using roto-tiller, throughout the year. Tillage operations were carried out frequently (maximum every two weeks) to avoid grass cover, keep bare soil, limit crust formation, and maintain constant soil conditions over time.
(3) Nectariferous (NF), or a mix of herbaceous species capable of attracting insects and thus favouring biodiversity in the inter-row (Table 1). Soil preparation and sowing operations were carried out in October. In addition, mowing was done once at the end of the winter and three times during the summer.
(4) Single tillage (ST). Mechanical weeding using roto-tiller was carried out in October, and then standard plant cover (i.e. the same grass and cover crops used in RF) was promoted during the year under study. Also for this management, the grass was cut in winter and three times in summer.

2.3. Field survey and measurement

2.3.1. Topographic data

The topographic data were obtained by a photogrammetric workflow based on drone images. The survey was carried out in February when the vines were still leafless and the terrain is more visible. It was performed with a professional quadcopter (DJI Matrice210v2), which was equipped with the DJI Zenmuse X4S camera (20 M pixels, focal length 8.8 mm, 1-inch CMOS sensor). The flight was conducted manually by a qualified pilot, ensuring optimal image overlap to improve matching performance in the SfM procedure (Eisenbeiss and Sauerbier, 2011; Eltner et al., 2016). The main characteristics of the flight are summarised in Table 2.

The images were pre-calibrated using Agisoft Lens® software, which allows calculation of camera model parameters and lens distortion coefficients to improve subsequent processing. The drone survey was supported by ground points with coordinates measured using a Geomax Zenith40 GNSS (Global Navigation Satellite System) in Real-Time Kinematic (RTK) mode (WGS84/UTM zone 32 N, EPSG: 32632). They were randomly distributed in the vineyard to avoid the formation of clusters or preferential lines. Specifically, Ground Control Points (GCPs) were used in the georeferencing and registration processes to improve the quality of the terrain reconstruction, while Check Points (CPs) were used to assess the quality of the topographic results. (Fig. 2).

The photogrammetric workflow was performed using Agisoft PhotoScan Pro® 1.4.5 software. It allows the calculation of a point cloud and high-resolution orthomosaic (0.025 m/pixel) from the images using the Structure-from-Motion (SfM) and Multi-Stereo-View (MSV) algorithms. The computation of point residuals, i.e. the bias between the value estimated by the photogrammetric process and the coordinates of the GCPs, was used to assess the uncertainty of the method. The mean of the residuals measures the accuracy of the registration process (if based on GCPs comparison) and the point cloud (using CPs). Standard deviation of the residuals could be used then to assess its precision (Cucchiaro et al., 2020). As proposed by Remondino et al. (2017), several evaluation methods could be performed. Widely used are the RMSE calculated on the three directions x,y,z ($RMSE_{3D}$), the planar direction ($RMSE_{xy}$) and the vertical direction ($RMSE_z$). The following Table 3a summarises the indicator purpose and shows the obtained values.

The dense point cloud, i.e. the output of the MSV algorithm, was subsequently imported into CloudCompare software (Omnia Version 2.10.2; http://www.danielgm.net) for filtering operations to remove vines and any points not belonging to the study area. This was done by manually cleaning the clouds and using a Statistical Outliers Removal (SOR) filter to remove noise while preserving surface features. After cleaning, the dense cloud was interpolated and gridded using the Natural Neighborhood algorithm in Esri ArcGIS® Desktop (version 10.6.1.9270) DEM creation software (0.05 m/pixel). This method was chosen because it limits the smoothing of the surface, preserving the microtopography (Pirotti and Tarolli, 2010). The DEM was also evaluated through specific metrics (Table 3b), to understand whether it was effectively suitable for the research. In particular, the elevation value of the DEM was compared with the coordinates measured on GCP and CP with GNSS following the method proposed by Höhle and Höhle (2009). After removing the outliers, RMSE (Estornell et al., 2011), standard deviation (SDE), mean error (ME), normalised median absolute deviation (NMAD) were calculated (Höhle and Höhle, 2009; Gonçalves et al., 2018; Cucchiaro et al., 2020).

To finish, from the high-resolution orthophotos (0.025 m/pixel), the

Table 2
Summary information about the drone survey.

Covered Area (ha)	Number of images	Average flight height (m)	Number of Tie Points	Ground resolution (mm/px)	Number of GCPs (CPs)	GNSS positional accuracy (x, y - z) (m)
0.57	563	15.5	5165,833	3.84	24 (10)	0.02–0.03

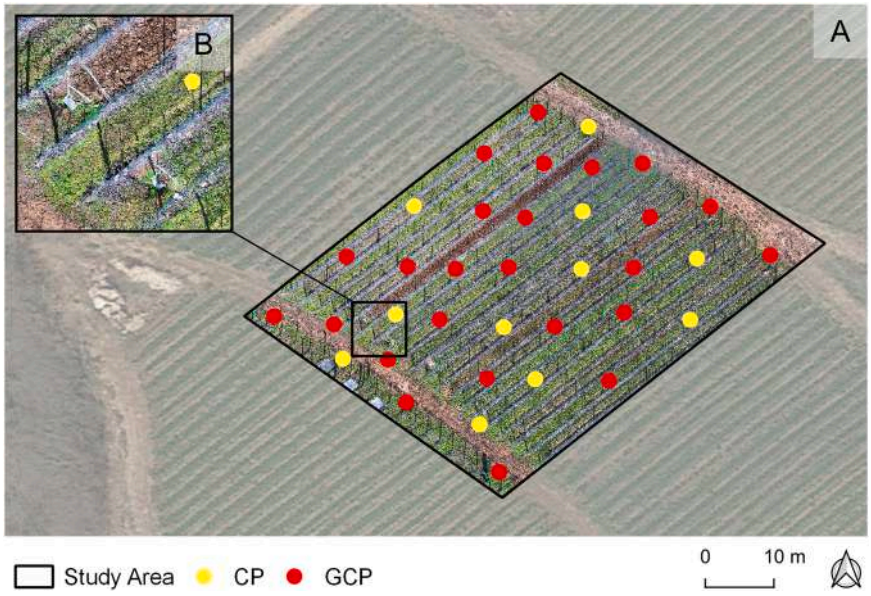

Fig. 2. Placement of the 11 Control Points (CPs in yellow) and 25 Ground Control Points (GCPs in red) distributed throughout the study area. (For interpretation of the references to colour in this figure legend, the reader is referred to the web version of this article.)

Table 3
Quality assessment of the produced point cloud (a) and Digital Elevation Model (DEM; b) in this study, showing values of mean absolute error (MAE), root mean squared error (RMSE), standard deviation (SDE), mean error (ME) and normalised median absolute deviation (NMAD).

(a) Point cloud assessment							
Accuracy CPs				Precision CPs			Registration GCPs
MAE (m)			$RMSE_{3D}$ (m)	SDE (m)			$RMSE_{3D}$ (m)
X	Y	Z		X	Y	Z	
0.018	0.014	0.011	0.023	0.007	0.006	0.007	0.024

(b) DEM assessment					
MAE (m)	ME (m)	SDE (m)	RMSE (m)	Median (m)	NMAD (m)
0.036	0.003	0.008	0.019	-0.001	0.005

polygons delimiting the various experimental inter-rows of the vineyard under different management were drawn, following the approach of Pijl et al. (2020). This operation produced the input rasters necessary for the SIMWE model to simulate runoff and sediment movement due to heavy rain (see Section 2.4). In addition to the polygon delimiting each management, polygons were identified in the proximity of Vines (VI) and areas compacted by the tyres of agricultural vehicles (or Wheel Tracks, WT). The latter was not drawn for CT, as the soil is continuously tilled to avoid compaction.

2.3.2. Rainfall analysis

The rainfall data used in this work were recorded by a weather station about 1500 m far from the study area and logged at a frequency of 5 min (ARPAV, 2020). The average annual precipitation over the last 27 years was 1308.8 mm (340 mm standard deviation) in 95 days of rain, mainly concentrated during spring and autumn. The rainiest month was November, with an average of 183.4 mm. In 2020, the total rainfall was 1271 mm distributed over 85 days, values in line with the historical trend. The highest rainfall intensity (5-minutes intervals) recorded in the study area was 182.4 mm h^{-1} during an extreme rainfall event during August (for further details on the event see a report recently posted on EGU blog: https://blogs.egu.eu/divisions/nh/2020/12/21/climate-change-is-viticulture-under-threat/). During the year, a total of 8 rainfall/runoff events (RE; Fig. 3) were recorded, showing that in sloping conditions surface runoff occurs quite commonly. It is worth noting that the number of events was similar to the research conducted by Bagagiolo et al. (2018), who recorded 72 events in 2 sites in 4 years, i.e. 9 events/year on average. Of the recorded precipitation, the least amount of rain that was able to generate runoff occurred in early June 2020, with 76.8 mm h^{-1}. According to the data collected, the combination of steep slopes, soil characteristics and consistent rainfall make the study area interesting for runoff and erosion investigation.

2.3.3. Infiltration rate

One of the main soil characteristics in terms of overland flow generation and soil erosion phenomena on agricultural fields is the infiltration rate. It varies according to the type of crop, soil and its compaction (Morin and Benyamini, 1977). There are several methods for its measurement. Lili et al. (2008) introduced four categories of infiltrability measurements, such as infiltration under unlimited water supply conditions, disc permeameter, linear source method and infiltration under rainfall conditions. For this research, saturated hydraulic conductivity was investigated using a double-ring infiltrometer following the methodology proposed by Lai and Ren (2007). The instrument consists of two metal rings with a diameter of 0.23 m (inner ring) and 0.52 m (outer ring), which are strong enough to be carefully forced into the ground concentrically to a depth of about 0.10 m. The two rings were then filled with water and the infiltration time was measured, repeating the operation until constant infiltration flow values were obtained. The procedure was repeated twice for each type of management investigated, as well as for areas close to vines and zones compressed by the transit of agricultural vehicles. In the case of CT, due

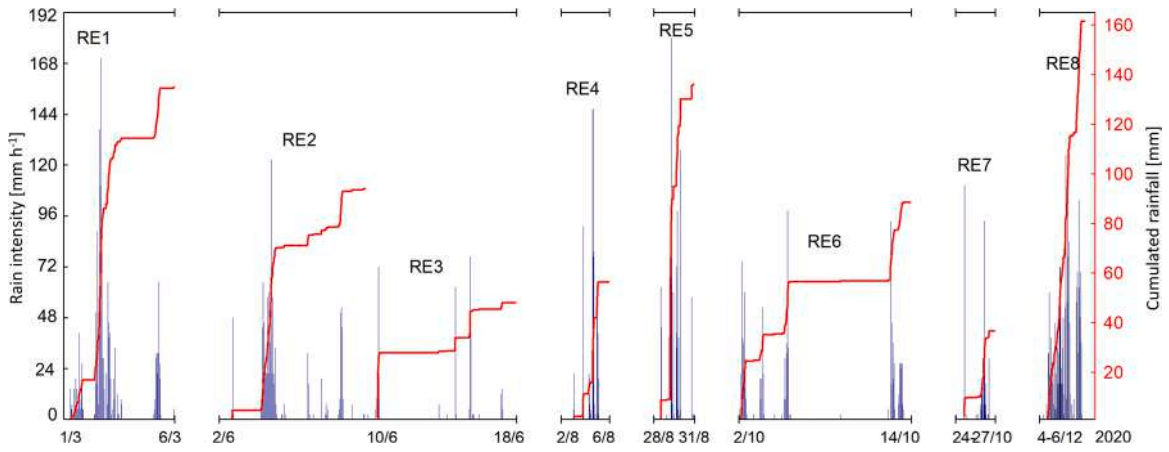

Fig. 3. Rainfall intensity (mm h^{-1}) and cumulated rainfall (mm) with a 5-min interval for the 8 rainfall/runoff events (RE) recorded in 2020.

Table 4
Field-measured infiltration rates (mm h^{-1}) and Manning's roughness coefficients (from Chow, 1959; Bunya et al., 2010) assigned to each of the specified land cover classes of this study: continuous tillage inter-row CT, reference inter-row RF, nectariferous inter-row NF, single-tillage inter-row ST, wheel tracks WT, and vine rows VI.

Parameter	CT	RF	NF	ST	WT	VI
Infiltration rate (mm h^{-1})	64.0	8.2	28.0	18.9	3.0	37.0
Manning's roughness coefficient (-)	0.030	0.035	0.035	0.035	0.030	0.100

to the high variability of post-tillage soil conditions (e.g. due to soil settling), the assessment of infiltration rate was carried out in a moment between two interventions to capture a representative soil condition for measurement. Infiltration values are expressed in the following section about SIMWE parameters (specifically in Table 4).

2.4. SIMWE model

In this research, the propensity of different types of management in the experimental vineyard to generate water runoff and subsequent soil erosion was assessed. To do this, the Simulation Water Erosion (SIMWE) model was used, developed by Mitas and Mitasova (1998). It is a physically-based model able to simulate the movement of soil particles due to overland flow generated by a single rainfall event (Li et al., 2020). Four precipitations were simulated (rain intensity in 5-minutes steps, expressed in mm h^{-1}), based on the rainfall values that generated runoff in the study area. The maximum simulated rainfall intensity (5-minutes steps) was 182.4 mm h^{-1}, the extreme event recorded in August 2020 (see section 2.3.2). In addition, four rainfall events of lower intensity were considered: 144 mm h^{-1}, 75.6 mm h^{-1}, which is the lowest reported intensity that generated runoff) and 48 mm h^{-1}, a rainfall event that did not generate runoff but is still relevant and potentially critical. SIMWE follows the principles of the Water Erosion Prediction Project (WEPP; Flanagan and Nearing, 1995) and was designed for complex soil, ground and cover conditions, therefore suitable for man-made landscape. To fully incorporate this variability, water and sediment flow as described as bivariate vector fields (Julien et al., 1995). Its ability to adapt to different spatial conditions was the reason why SIMWE was chosen in this research. Indeed, other authors propose it for similar objectives. For example, Pijl et al. (2020) used it to simulate the erosion rate in several vineyards, one of which has similar management characteristics for this work's study area (steep slope arranged with up to down rows covered by grass).

SIMWE is divided into two components, both implemented in *GRASS GIS* tools. The first one aims at simulating the surface runoff (*r.sim. water*), i.e. a shallow water flow described in the model by the bivariate form of the Saint Venant equations (Mitas and Mitasova, 1998). The model requires a rainfall intensity value (mm h^{-1}), soil infiltration rate (mm h^{-1}), digital elevation model (m) as well as its first-order derivative in x and y (-), and the Manning's roughness coefficient (-). The main inputs used are reported in Table 4.

This model's component offers as outputs a spatialised value of the runoff water depth (m) and its discharge (m^3 s^{-1}). These results are then implemented as input in the second model's component regarding the transported sediment analysis (*r.sim.sediment*), which is quantified by relating it to the overland flow respecting the continuity of sediment mass (Neteler and Mitasova, 2008). Other inputs are topographical information (DEM and its first-order derivates in x and y, same for r.sim. water), Manning's roughness coefficient (-), and soil specifications such as detachment capacity coefficient (s m^{-1}), transport capacity coefficient (s) and critical shear stress (Pa). The last three parameters of the model were not calculated directly by in-field observations but were assumed by using the values proposed by the model's authors for a similar scenario (0.001 s m^{-1}, 0.001 s and 0.5 Pa respectively). Other research has successfully adopted a similar methodology in vineyards located in the same region (Pijl et al., 2020), obtaining values in line with Fernandes et al. (2017) for a Portuguese site. Although this is a limitation in the quantification of the erosion/transportation processes, the aim of the study is the comparison of inter-rows located in the same vineyard with a low-cost methodology, which is why we consider the implementation of tabular literature values to be sufficiently robust for the purpose. SIMWE offers many outputs related to sediment transportation, including sediment transport capacity (kg m^{-1} s^{-1}), flux (kg m^{-1} s^{-1}), concentration (particles per m^3) and net erosion/deposition (kg m^{-2} s^{-1}).

The outputs of the SIMWE model investigated in this research are water discharge for the first component and sediment concentration for the second. The first allows understanding the overland flow process occurring in the vineyard, while the second offers an insight into how much sediment is transported by it (Mitasova and Mitas, 2001). A comparison of the results obtained in the different experimental inter-rows allows an understanding of the runoff and soil erosion phenomena in steep slope vineyards. In addition to the maps displaying the model's outputs, *Probability Density Functions* (PDFs) are calculated to provide a clearer overview of rasters' distributions, as well as facilitating the comparison between various managements. Outcomes could be used to offer cost-effective guidelines to stakeholders for more sustainable management. Finally, SIMWE model results were statistically compared using (1) a one-way ANOVA test to capture significant differences between soil management and (2) a post-hoc Tukey-Kramer test to perform pairwise comparisons.

The selected model simplifies the process of water infiltration into the ground by assuming a saturated soil condition and a vertical steady-

state water flow, therefore suitable for fairly deep soils such as the one in the study area (see Section 2.1). Model simulations were also analysed both in-situ (the entire interrow) and ex-situ (the lowest 1-m cross section of the interrow) to investigate if downstream impacts were in line with internal processes.

2.5. Index of connectivity

The Index of Connectivity IC was used in this research to identify specific patterns in terms of sediment connectivity in the four inter-rows tested through different management. The index used was proposed by Borselli et al. (2008) and modified by Cavalli et al. (2013), following the Eq. (1):

$$IC = \log_{10}\left(\frac{D_{up}}{D_{dn}}\right) \quad (1)$$

IC ranges from + ∞ to -∞ and as the index value increases, the degree of connectivity also rises. D_{up} is the routing potential undergone by sediment produced in the contributing area. It is a function of the slope gradient and soil roughness. D_{dn} depends on the length of the path followed by runoff and sediment moving from the source area to a target (in this research, the area downstream of the single experimental inter-rows). It varies according to the length and slope of the path and the terrain roughness. IC was calculated using the *SedInConnect 2.3* stand-alone application proposed by Crema and Cavalli (2018) on the DEM derived from UAV-SfM of the study area and its roughness as a weighting factor.

It was employed for the identification of possible typical pathways followed by runoff/sediments in the different managements under study. Specifically, the index was calculated with the aim of assessing the role of areas compacted by the transit of agricultural vehicles in providing a preferential pathway for runoff and sediment, and to observe the role of tillage in mitigating the problem. In this work, the IC related to each practice was also quantified using a Probability Density Function. Additionally, two statistical tests were carried out. Firstly, IC values related to each practice were compared for significant differences using the post-hoc Tukey-Kramer test. Secondly, a one-way ANOVA test was used to determine significant differences between IC found in wheel tracks and IC outside of these for all practices combined.

2.6. In-field observations

The work aims to verify which type of inter-row management most effectively mitigates the negative effects of heavy rainfall, an important issue in a climate change perspective. To do that, this paper proposes a modelling approach for understanding the runoff and sediment phenomena in a steep slope vineyard managed under different soil practices. To support the model outcomes, a collection of surface runoff and sediment samples generated following heavy rainfall was carried out. This was performed by implementing a low-cost collection system downstream of the study inter-rows (Fig. 4 illustrates the process). The function of the system was not a formal quantification of hydrological and erosion processes, as proposed by other researchers, which used more complex and expensive systems for longer periods (Biddoccu et al., 2016). Following the approach of Carretta et al. (2021), we applied a cost-effective and low-impact methodology for verifying similarities between simulated outcomes and in-field observations. Specifically, downstream of the inter-rows understudy, boxes were inserted into the ground, with dimensions of 560*410*395 mm. Upstream from each box, two metal bars with angular profiles of 1 m in length were used to function as drainage channels, which drained the water and sediment inside. Furthermore, to intercept the water coming from the central part of the inter-row, a longitudinal metal bar was installed to convey the fluid into the two drains. Finally, to avoid bias in the data due to rainwater, the box was constantly covered with a shelter, ensuring that all the water in the box was the result of the runoff process. Before starting the measurements, the system was tested to minimise water and sediment losses due to design limitations and to ensure that the conditions were the same for each management studied, guaranteeing comparability of collected data. In addition, the entire system was constantly maintained with weekly routine maintenance during data collection. Finally, during data collection, attention was paid to ensure that the collection box was never full of water, to avoid an overestimation of sediment quantification at the end of the event (with a tank full of water, but with a constant runoff input, the volume of water remains the same, while the amount of sediment would increase distorting the results). Following heavy rainfall, which generated a sufficiently consistent runoff to be collected in the system, a sample of water and sediment was collected. First, the collected solution was stirred, promoting a homogeneous suspension of the sediment in the water. Next, a one-litre sample was collected and left for roughly ten days in the laboratory, waiting for the deposit of the material on the bottom. By measuring the

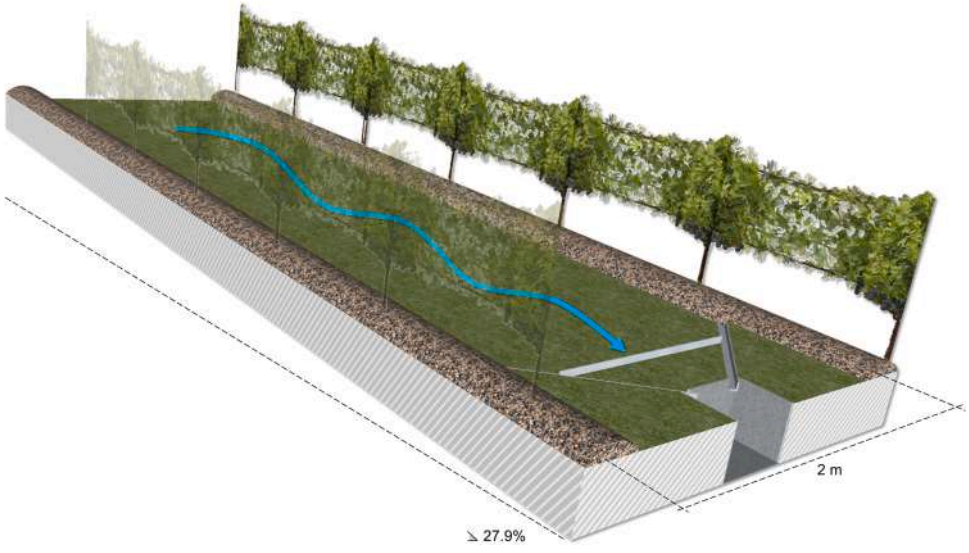

Fig. 4. Graphical render of an inter-row of the experimental vineyard of the research. Downstream, the structure for runoff interception is shown, which collected the water in a sub-soil box.

proportion of sediment volume to total volume using a measuring bar, the percentage of sediment in the collected solution was estimated. Finally, a further confirmation was made by comparing these values with simulations of sediment concentration ex-situ (i.e. in the last metre of each row).

3. Results and discussion

3.1. Assessment of overland flow

The physically-based model SIMWE was used to simulate the runoff and soil erosion dynamics occurring in the vineyard in the four experimental inter-rows. The *water discharge ($m^3 s^{-1}$)* output of the first model's component was used to describe the overland flow process in terms of fluid component (*r.sim.water*, see Section 2.4 for further details). It was spatialised through a raster offering an intuitive understanding of the process along the study area. Specifically, four rainfall events of increasing intensity were simulated. This allowed appreciating the hydrological response of the inter-rows under conditions of ordinary rainfall (48 mm h^{-1}; nine events recorded with rainfall between 42 mm h^{-1} and 54 mm h^{-1}), and increasing severity (peaks above 144 mm h^{-1}; events occurred more rarely – 2 records; see Fig. 3). The result of the shallow overflow simulations is shown in Fig. 5 (A to D). Transparent colour is set for areas where no runoff occurs, while blue to white colours are associated with increasing runoff outcomes. In addition, for each simulation, the Probability Density Function (PDF) is shown together with the map to better understand the distribution of typical discharge values for each of the four tested managements.

In the first simulation of 48 mm h^{-1}, effective performance by continuous tillage (CT) in limiting the formation of runoff is noticed (different transparent spots along the inter-row are visible). This aspect was determined by a better infiltration capacity of the soil compared to the other management, ensuring a lower fraction of surface water to flow downstream. However, this is a temporary effect and usually noticeable only in the post-tillage period (Buesa et al., 2021; Triplett and Dick, 2008). In addition, CT is susceptible to crusting, especially during the warmer months, which limits infiltration by causing runoff (Myers and Wagger, 1996). To investigate a soil management approach capable of preventing this problem, we scheduled high-frequency tillage. In this way, it was possible to keep the soil consistent over time, allowing the use of a representative infiltration rate value as model input. In the simulations, a positive effect of infiltration rate is also visible in the upstream part of single tillage (ST), which subsequently shows a uniform pattern of overflow along the inter-row. A similar situation is observed for nectariferous crops (NF), wherein the upstream part of the vineyard runoff is almost null, increasing downstream in a less uniform way, showing some spots at higher flow rates. The management with the greatest simulated water flow is the reference (RF). Although less runoff is observed near the sides of the inter-row (where the infiltration effect of the soil close to the vine mitigates the process), the central part is characterised by higher discharge values. As the intensity of precipitation increases, the runoff conditions become more uniform between the various management systems. This is visible in PDFs, where the vertical lines representing the median of the distributions tend to assume comparable values. This was due to the decreasing weight of soil infiltration capacity, which plays a diminishing role at higher rainfall rates. In general, for extreme rainfall and referring to the water component only (sediment is discussed in section 4.2), CT is the system that generates the least surface water flow, while higher flow values are observed in RF. Furthermore, median values of discharge are similar for NF and ST, with the post-hoc statistical tests showing no significant difference (p-value $<$ 0.01). However, it is important to underline that these results only take into account the water component and not the sediment component, a fact shown and discussed in the next Section 4.2.

3.2. Assessment of sediment concentration

The second component of the SIMWE model (r.sim.sediment) was used to simulate the concentration of sediment transported by the runoff (particle m^{-3}). By describing the amount of sediment transported by the overland flow and generated by an input of rain, it is possible to evaluate which management can better mitigate soil erosion due to extreme rainfall. As in the case of the first SIMWE component, four rainfall/runoff events of increasing intensity were simulated. In this way, the result offers a view of sediment production for ordinary precipitation (more frequent during the year) and extraordinary rainfall (less frequent, but more impactful in terms of erosion). The result is shown in Fig. 6 A-D below. It is themed in increasingly lighter colours for higher sediment concentrations. In addition, it proposes a PDF beside each map to graphically illustrate the values' distribution.

First of all, it can be seen that for each simulated rain, the sediment concentration tends to be highest in CT. This is because of the lack of grass cover, which offers active protection to soil particles (Szögi et al., 2007; Marques et al., 2010). Indeed, despite the runoff rate (liquid component) tends to be lower in CT compared to other management thanks to better infiltration rates, the sediment concentration proved to be of greater magnitude. This fact was observed by several authors, who have emphasised the role of grass cover in mitigating soil loss on steep slope vineyards (Blavet et al., 2009; Morvan et al., 2014; Biddoccu et al. (2016)).

The behaviour of the different management systems in generating sediment at different rainfall intensities is another interesting theme observed in the results of the simulations. For the lower rainfall intensities (48 mm h^{-1}) the highest concentration of sediment for grass-covered inter-rows is found in RF. The better performance of ST and NF is likely related to a generally greater infiltration rate, which limits the formation of runoff, a fact that can be observed in Fig. 6. This underlines the relevance of areas where the soil is compacted due to the transit of agricultural vehicles, which tends to increase runoff occurrence due to reduced hydraulic conductivity (Ferrero et al., 2005; Capello et al., 2017) and due to the formation of preferential pathways in the slightly lower tracks (Pijl et al., 2021). This is also the reason why it was chosen to calculate the sediment connectivity index (see Section 2.5), in which the role of these areas in terms of source of sediment is researched and discussed. On the other hand, as the intensity of rainfall increases, similar values of sediment concentrations were found in the three grass-cover managements RF, NF, ST. In general, for the two simulations with central rainfall values (75.6 mm h^{-1} and 144 mm h^{-1}) the management that produced the lowest sediment concentration is ST. For the most extreme rainfall simulated (182.4 mm h^{-1}), NF and ST assume a similar sediment concentration value (p-value $<$ 0.01).

Field-measured sediment concentration values are reported in Table 6, expressed in proportional terms of deposited sediment depth out of total depth sampled from the collection boxes. Averages are provided for each practice, as well as a relative difference of CT, NF, and ST practices compared to the reference RF in percent. Sampled concentration values are relatively homogeneous with limited standard deviations (ranging from 0.003 to 0.008 particle m^{-3}) between the 8 rainfall events (RE1-RE8, Fig. 3), indicating good consistency of the applied method. The internal variability of sediment load for each practice can be related to the intensity of rain events (Fig. 3), e.g. with RE1, RE4 and RE5 corresponding to the highest values, and RE3 corresponding to the lowest values. Strikingly, the relative differences of sampled sediment concentration of the four practices (Table 6) are similar to the simulated differences (Table 5), with CT showing 82% more measured sediment than the RF, whereas NF and ST respectively showing 36% and 53% less measured sediment (compared to +92%, −40%, and −57% in the simulations). This provides a measure of confidence in model performance, at least for the purpose of comparing between practices. The most notable deviation of simulated values (Table 5) is a 5–10% overestimation in the CT, NF, and ST practices

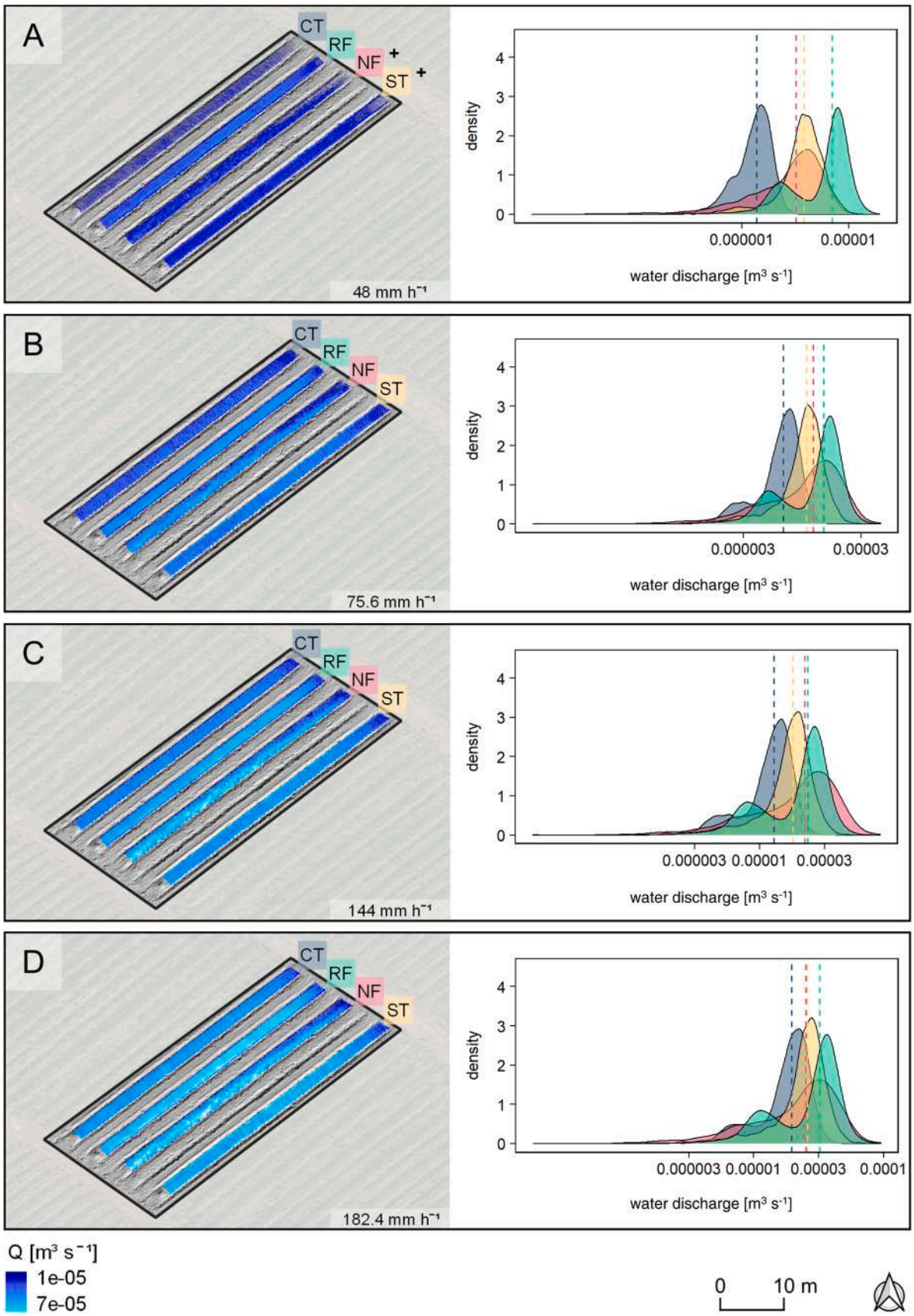

Fig. 5. Simulated discharge ($m^3\ s^{-1}$) under four rainfall scenarios with increasing intensity (A-D), for each showing the spatial distribution of flow throughout the 4 inter-rows under practices of continuous tillage CT, reference RF, nectariferous NF, and single-tillage ST (left panels), as well as the probability density function of each scenario (right panels, median values indicated by dashed lines). Post-hoc significance testing (Tukey-Kramer) revealed that NF and ST practices were statistically indifferent in the first scenario (plus-symbol).

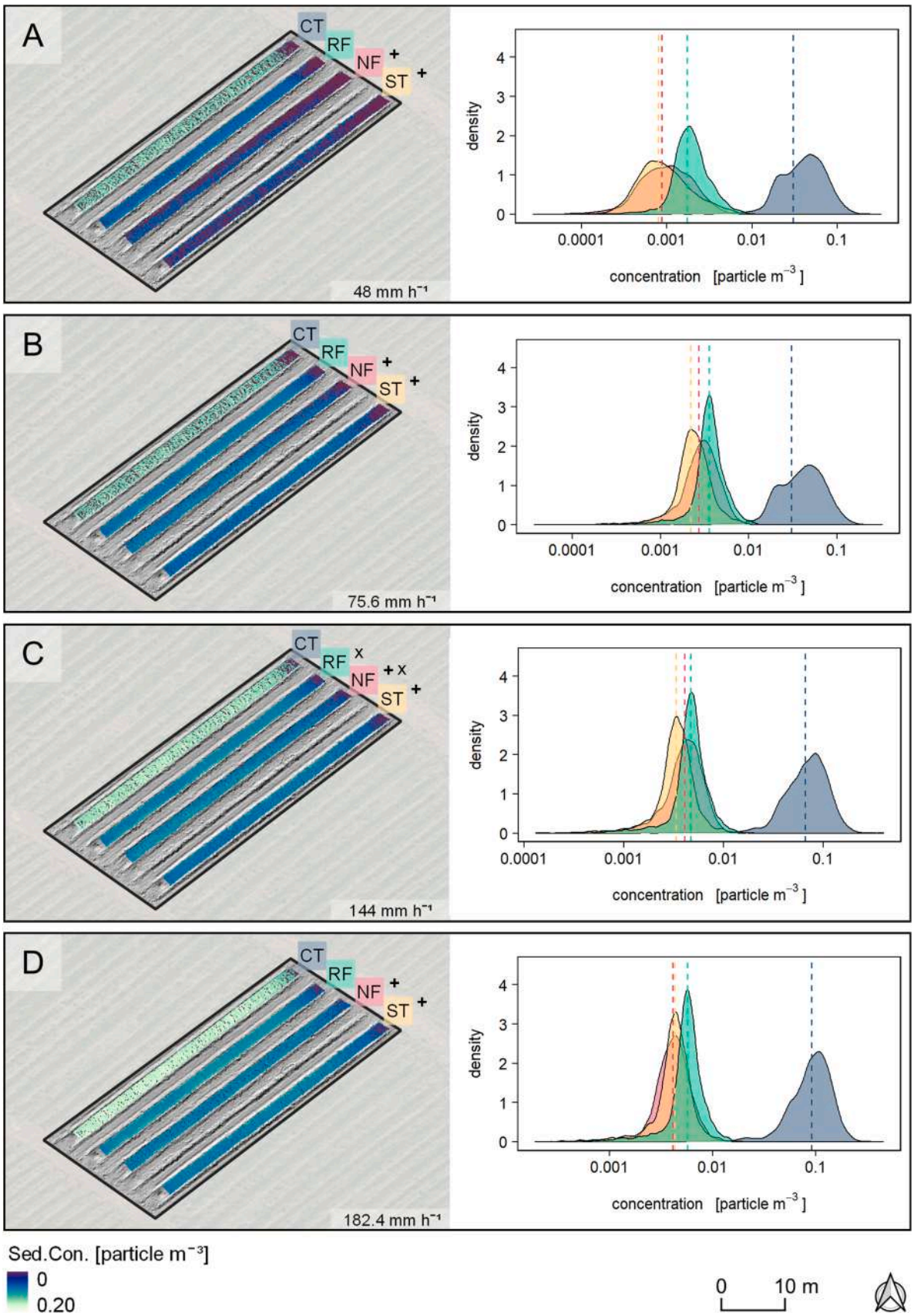

Fig. 6. Simulated sediment concentration (particle m^{-3}) under four rainfall scenarios with increasing intensity (A-D), for each showing the spatial distribution of flow throughout the 4 inter-rows under practices of continuous tillage CT, reference RF, nectariferous NF, and single-tillage ST (left panels), as well as the probability density function of each scenario (right panels, median values indicated by dashed lines). Post-hoc significance testing (Tukey-Kramer) revealed that NF and ST practices were statistically indifferentiable for each scenario (+ symbol) while RF and NF were indifferent in the same scenario (x-symbol).

Table 5
Median and standard deviation values of simulated discharge ($m^3 s^{-1}$) and sediment concentration (particle m^{-3}) under the four rainfall scenarios and four inter-row practices continuous tillage CT, reference RF, nectariferous NF, and single tillage ST. Additionally, relative changes of CT, NF and ST as compared to reference RF are provided as percentages.

Rain [mm h-1]	Water discharge [$m^3 s^{-1}$]						
	RF	CT		NF		ST	
48	7.03E-06 ± (3.09E-06)	1.37E-06 ± (4.71E-07)	-415%	3.20E-06 ± (1.91E-06)	-120%	3.83E-06 ± (1.67E-06)	-84%
75.6	1.52E-05 ± (6.53E-06)	6.88E-06 ± (2.47E-06)	-121%	1.23E-05 ± (7.40E-06)	-23%	1.08E-05 ± (3.99E-06)	-40%
144	2.35E-05 ± (1.00E-05)	1.29E-05 ± (4.68E-06)	-82%	2.23E-05 ± (1.34E-05)	-5%	1.81E-05 ± (6.41E-06)	-30%
182.4	3.22E-05 ± (1.37E-05)	1.95E-05 ± (7.08E-06)	-65%	2.51E-05 ± (1.51E-05)	-28%	2.58E-05 ± (9.09E-06)	-25%
	Sediment concentration [particle m^{-3}]						
48	1.73E-03 ± (1.31E-03)	3.03E-02 ± (3.08E-02)	+ 94%	9.90E-04 ± (8.30E-04)	-75%	9.00E-04 ± (9.43E-04)	-92%
75.6	3.55E-03 ± (1.75E-03)	3.03E-02 ± (3.08E-02)	+ 88%	2.71E-03 ± (1.71E-03)	-31%	2.19E-03 ± (1.48E-03)	-62%
144	4.72E-03 ± (2.02E-03)	6.59E-02 (4.03E-02)	+ 93%	4.06E-03 ± (2.04E-03)	-16%	3.34E-03 ± (1.70E-03)	-41%
182.4	5.68E-03 ± (2.22E-03)	9.12E-02 (4.61E-02)	+ 94%	4.10E-03 ± (1.87E-03)	-38%	4.26E-03 ± (1.91E-03)	-33%
	average difference with RF:		*+ 92%*		*-40%*		*-57%*

Table 6
Proportional sediment concentration (deposited soil depth / total depth) for each practice, as sampled from the collection boxes during the 8 rainfall/runoff events (RE1-RE8, see Fig. 3). In addition, the average concentration is provided for each practice, as well as the percentual difference with reference practice RF.

Event	RF	CT	NF	ST
RE1	0.031	0.057	0.018	0.016
RE2	0.027	0.038	0.019	0.013
RE3	0.019	0.039	0.01	0.008
RE4	0.029	0.061	0.013	0.011
RE5	0.033	0.052	0.023	0.013
RE6	0.021	0.041	0.019	0.017
RE7	0.022	0.037	0.013	0.008
RE8	0.025	0.051	0.018	0.012
Average	0.026	0.047	0.017	0.012
(± st.dev.)	(± 0.004)	(± 0.008)	(± 0.004)	(± 0.003)
average difference with RF:		*82%*	*-36%*	*-53%*

(compared to RF), which is causing a mild uncertainty to the impact quantification presented in this section. This could be attributable to intrinsic limitations of the physical model, which uses, for reasons related to the type of approach sought, some input data from literature and not directly calculated in the study area.

A limitation could be found in low-cost sample analysis. While measuring the layers of water and deposited sediments, the fraction of water contained within the sediment micropores was not accounted for. However, this bias was negligible thanks to the very fine grain size of the sediment. Nevertheless, this effect is consistent across all practices. The technique selected to measure sediment concentration is reasonably simple and cost-effective. Therefore, it is suitable for application in different contexts around the world, even in rural areas with poor infrastructure and where instruments, resources, and specialised personnel are lacking. For this reason, an estimation of the values was therefore sufficiently adequate for the scope of this work, in support of the results obtained from the physically-based model.

With regards to the boundary condition assessment, ex-situ discharge values were consistent with the in-situ processes, with lower average discharge in CT than RF and in grass-covered practices ST and NF. This behaviour was also observed for sediment concentration, with higher averages in CT than RF (+112%) and uniformly lower values in NF (−52%) and ST (−49%). In addition, slightly higher average sediment concentration could be observed in the simulated ex-situ flow than in-situ (+13%) deviating from field measurements by 17%, and therefore compatible with the scope of this work.

3.3. Index of connectivity and impacts of mechanisation

The results presented in Section 4.2 show that among grass-covered managements, RF was the most problematic in terms of soil erosion phenomena. For this reason, it is important to investigate how the sediment source is connected to the downstream portion of the vineyard to detect preferential pathways using the connectivity index (CI). The following Fig. 7 shows the result obtained along the four experimental inter-rows and calculated based on the DEM derived from UAV-SfM (see Section 2.5 for more details). In the map, the index is themed by blue (less connected areas in terms of sediment connectivity) to red (for more connected areas) according to Cavalli et al. (2013). Other studies proposed a similar approach to describe sediment connectivity in vineyards at different spatial scales. For example, Prosdocimi et al. (2017) suggested the use of CI at the micro-plot level to understand soil erosion due to heavy rainfall (simulated using sprinklers) and by analysing which areas are most likely to produce the sediment, subsequently collected in appropriate containers. On a larger scale, Rodrigo-Comino et al. (2020) proposed the use of IC in a vineyard in Spain, where authors integrated in-situ measurements with IC to analyse the soil erosion process. Looking at the map in Fig. 7, the base of the vineyards is characterised by higher connectivity values than the upper part, but of greater interest is the analysis of the patterns that characterise each management. To better understand this phenomenon, a PDF showing the distribution of the index of connectivity's values for each management is proposed. In general, higher values (in terms of median) of the distribution were found in RF, while lower values in CT (the four distributions are significantly different; p-value < 0.01). The best performance of the latter is attributable to the micro-roughness of the continuously ploughed surface. In fact, looking at the map in Fig. 7, it is possible to notice a pattern in the centre of the inter-row with higher values of connectivity. This index behaviour is also similar for ST, which is also characterised by a surface treatment in the months preceding the UAV-SfM survey. Instead, in RF the situation is different. Two preferential paths are visible laterally to the inter-row, in correspondence with the areas subjected to soil compaction due to mechanisation. This shows that these sections of the inter-row are the most connected in terms of sediment connectivity and thus more critical. Indeed, these areas are potentially prone to the occurrence of soil erosion and sediment transport downstream. A significantly higher connectivity value was found in these areas if compared with the other part of the vineyard (p-value $<$ 0.01). Similar pathways, but of lower magnitude, are observed in NF, proving that also in this management it is possible to recognise in the surface microtopography the signature of the transit of agricultural machinery used for routine operations on the vines. Finally, it is worth pointing out that the application of the IC index is interesting in identifying the preferential pathways followed by water and sediment along the experimental inter-rows, not in comparing the sediment produced. In particular, the CI emphasised the central role of mechanisation in steep vineyards with regard to sediment transport processes, identifying critical areas in tractor tyre tracks.

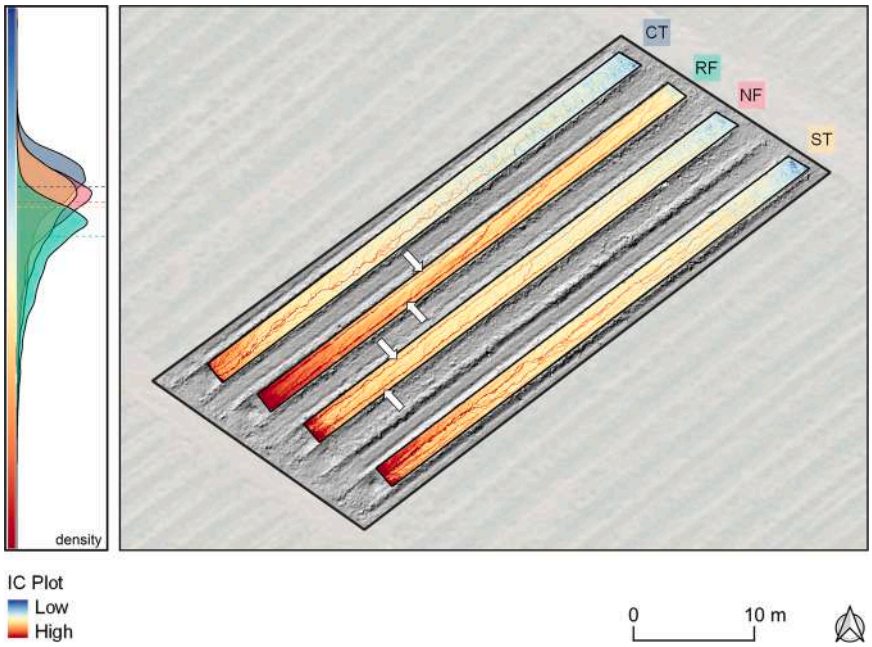

Fig. 7. Index of connectivity (IC) computed for the four inter-row practices of continuous tillage CT, reference RF, nectariferous NF, and single-tillage ST (right panel), also showing the distribution of each in a probability density function (left panel, median values indicated by dashed lines). Post-hoc Tukey-Kramer statistical testing showed that each practice had significantly different IC values. High connectivity values (in red) are visible in the parallel wheel tracks created by tractor passage in practices RF and NF (indicated by the arrows; significantly higher IC according to a one-way ANOVA test), indicating the impact of machinery on the formation of preferential pathways. (For interpretation of the references to colour in this figure legend, the reader is referred to the web version of this article.)

3.4. Final remarks

The applied methods proved to be valid in offering a general insight regarding the soil erosion process in a steep-slope vineyard managed with different soil managements. However, the work is characterised by some intrinsic limits that are inevitable but acceptable considering that complex phenomena are described with an expeditious and cost-effective methodology. We opted for the use of a physically-based model but researching low-cost inputs, the reason why some limitations could be found, such as in the use of literature values not calculated for the specific site. Another issue is the spatial accuracy of the input data. For example, instrumental and methodological errors could affect the quality of the UAV-SfM topographic survey (Sanz-Ablanedo et al., 2018). Since the DEM is the starting point for the simulation of runoff/erosion processes, residuals propagated from the point cloud to the DEM through interpolation and gridding operations affect the final accuracy of the results. Although these problems could be mitigated by a more intensive photogrammetric survey (for example with a larger photographic dataset and at a lower operational altitude of the drone), we consider topographical data adequate for the scope of the work. Similarly, the infiltration rate calculated for different coverages could also be affected by limitations. Firstly, we adopted a homogeneous infiltration rate for each class (such as continuous tillage, wheels tracks, etc.). Other limits concerned the instrumental error of the double ring infiltrometers, an effective and relatively easy-to-use instrument. However, several authors use it for similar purposes (Biddoccu et al., 2016; Peyrard et al., 2016), also for sloping surfaces (Bodhinayake et al., 2004), offering results in line with other literature values (Pijl et al., 2020). Finally, the water and sediment samples collected in the experimental boxes are also subject to limitations. For example, the measurement of the sediment concentration did not include complex laboratory analyses but consisted of a volumetric estimation of the sediment to the water.

The SIMWE model was already successfully applied and validated within the same wine-producing region following a similar workflow. Pijl et al. (2020) used it to investigate hydro-erosive processes in a comparable vineyard (cultivation along the slope and use of agricultural machinery) providing model validation through detailed in-field observation that confirmed the accuracy of the simulations. However, the proposed research aims to assess a diverse range of surface processes occurring in multiple soil management systems, and not to accurately quantify their individual magnitudes. Therefore, the impact of potential bias related to the model is negligible, as it is systematically repeated in the various simulations not compromising a diagnostic comparison. This approach was also pursued by Pijl et al. (2022). The authors explored the effect of vineyard configuration on runoff and soil erosion using the SIMWE model in the same wine production zone.

The simulations results were consistent with what was observed through the experimental plots. In general, the two types that proved to be most interesting in mitigating erosion in high slope vineyards were NF and ST. Both showed good performance in reducing material transported by runoff generated by heavy rainfall when compared to RF. In NF, the simulated sediment concentration reduction is around 40% (about 35% estimated from field samples). This is explained by a better infiltration capacity of water into the soil, favoured by a soil preparation in October and less sediment connectivity downstream. The nectariferous mix is also interesting since growth and soil cover in mid-autumn is very fast, and soon after winter, the cover is already complete reducing the risk of runoff/erosion. In addition, although it is not the main focus of the work, it is important to mention the ability of the nectariferous mix to provide flower-rich inter-rows that attract pollinating insects and favour a general development of biodiversity in the vineyard, that could positively affect ecosystem services (Paiola et al., 2020). The most effective erosion mitigation performance was observed in ST, with a simulated reduction in sediment concentration of roughly 57% compared to RF (approximately 52% estimated from field samples).

An interesting assessment can be made regarding the timing, i.e. the optimal moment of the year in which working should be done to mitigate soil erosion. In our case, single tillage was carried out in autumn, eliminating tractor tracks and favouring subsequent grass growth and infiltration in soil, ensuring limited runoff formation. In the case of climatic situations that concentrate prolonged rainfall with higher rainfall erosivity values during this season, it may be interesting to modify the scheduling of single tillage. An example could be the one reported for northern Italy by Biddoccu et al. (2016), where a higher presence of runoff and erosion yield was mainly due to November rainfall. In similar cases, it might be interesting to perform the tillage in late winter to prepare the surface for the interception of possible snowmelt runoff (mainly observed in February by Biddoccu et al.,

2016). Spring conditions would favour rapid grass growth protecting the soil from summer storms and during autumn, where higher erosion yields occur. Finally, as far as CT is concerned, management has not proved to be a valid RF alternative. Although it could offer a temporary benefit in mitigating overland flow formation and a lower IC, it was the management with the highest sediment concentration observed. Indeed, previous research highlighted the propensity of similar management to accelerate the erosion rate (Novara et al., 2019).

4. Conclusion

Runoff and soil erosion are processes that pose a serious threat to steep slope vineyards around the world. Climate change often aggravates the meteorological conditions of the areas where they are located, increasing the frequency of heavy rainfall, with serious consequences for the entire hilly and mountainous farming sector. Moreover, modern viticulture often prefers cultivation along the slope to favour mechanisation, which accelerates surface processes that cause erosion. For these reasons, sustainable management practices able to mitigate runoff and erosion are crucial in agricultural landscapes. Several studies focus on testing diverse inter-row soil practices able to balance the needs of vine cultivation with soil protection from the erosive effects of water. Often, they focus on in-field experiments, sometimes covering several years and using complex monitoring systems. In this work, the behaviour of four inter-row steep slope vineyard practices in generating runoff and soil erosion due to heavy rainfall is investigated. We opted for a modelling approach using a physically-based model (SIMWE) employing easily measurable and cost-effective input data. This workflow was successfully adopted by other authors in a similar vineyard in the same wine production area, providing outcomes validation based on field observations. The research tries to overcome time-consuming and expensive in-field quantifications, becoming attractive in different contexts, including developing countries. This was possible thanks to considerable technological innovation in recent decades, specifically in remote sensing. Indeed, new land surveying techniques offer high-resolution data that can be used for modelling applications, such as the UAV-SfM used in this work.

This research illustrates that in a steep mechanised vineyard cultivated along the slope, surface runoff and soil erosion due to heavy rainfall are significant issues. Outcomes show that a single tillage (ST) mitigates the soil erosion process in steep slope vineyards, in comparison with grassed but untilled management widely used in northern Italy (RF). In addition, good performance was observed from the use of a mix of nectariferous herbaceous species (NF), which combines the positive effects of soil preparation with a flower development that favour biodiversity. Furthermore, the unsustainability of continuous tillage (CT) in terms of erosion yield was assessed, producing the highest concentration of sediment in the runoff. The modelling results were compared with water and sediment samples collected in the field after heavy rainfall. The collection method used was low-cost, easy to install and potentially applicable in many different contexts, the basic philosophy behind this work. Although this method provides a rough estimation of sediment concentration, it was suitable for research purposes. Finally, the work shows how the application of a connectivity index processed on high-resolution remote sensing data can be useful to understand the impact of mechanisation in vineyards. Specifically, maximum values of IC were found in mechanised soil management (mainly in NF) and in correspondence of tyre tracks.

In conclusion, research outcomes show that a low-cost modelling-based approach, which avoids expensive analyses for data collection, allows obtaining interesting information in runoff and soil erosion assessment. The method could be systematically replicated in different areas of the world to support the optimal and targeted choice of soil management to mitigate erosion in steep-slope vineyards. Specifically, with a future in which critical scenarios due to climate change are projected, it is important to prepare in advance and with a prevention perspective, creating methods and guidelines for finding sustainable solutions.

Funding

This study was partly supported by the project SOiLUTION SYSTEM "Innovative solutions for soil erosion risk mitigation and a better management of vineyards in hilly and mountain landscapes", within Programma di Sviluppo Rurale per il Veneto 2014–2020 (Italy; www.soilutionsystem.com).

CRediT authorship contribution statement

Eugenio Straffelini: Conceptualisation, Methodology, Formal analysis, Data curation, Writing of original draft. **Anton Pijl:** Conceptualisation, Methodology, Formal analysis, Data curation. **Stefan Otto:** Data collection in the field, Methodology. **Enrico Marchesini:** Data collection in the field. **Andrea Pitacco:** Methodology. **Paolo Tarolli:** Conceptualisation, Review and editing, Funding acquisition, Project administration, Supervision, Principal investigator.

Declaration of Competing Interest

The authors report no declarations of interest. The authors declare that they have no known competing financial interests or personal relationships that could have appeared to influence the work reported in this paper.

Acknowledgements

The authors would like to thank the farms 'Azienda agricola Gini Sandro e Claudio' and 'Azienda agricola Coffele' for making their vineyards available for the research, the Consorzio Tutela Vini Soave e Recioto di Soave, the Consorzio Volontario di Tutela del Vino Lessini Durello D.O.C., the pilot Dr. Sara Cucchiaro (Post-doctoral researchers at the University of Padova) for flying the drone during the photogrammetric survey, and Wendi Wang (PhD student at the University of Padova) and Simone Gottardi (Agrea s.r.l) for their precious support in the field operations.

References

Alewell, C., Borrelli, P., Meusburger, K., Panagos, P., 2019. Using the USLE: chances, challenges and limitations of soil erosion modelling. Int. Soil Water Conserv. Res. 7, 203–225. https://doi.org/10.1016/j.iswcr.2019.05.004.

Angulo-Jaramillo, R., Bagarello, V., Iovino, M., Lassabatere, L., 2016. Infiltration Measurements for Soil Hydraulic Characterization. Springer. https://doi.org/10.1007/978-3-319-31788-5.

ARPAV, 2020. Principali variabili meteorologiche - Anni 1994–2019. ⟨https://www.arpa.veneto.it/dati-ambientali/open-data/clima/principali-variabili-meteorologiche⟩ (accessed 2.2.21).

ARPAV, 2019. Carta dei Suoli del Veneto in scala 1:250.000 - Versione 2019. ⟨https://www.arpa.veneto.it/temi-ambientali/suolo/conoscenza-dei-suoli/carta-1–250.000/leg_250k.pdf⟩ (accessed 2.2.21).

Arriola-Valverde, S., Villalobos-Avellan, L.C., Villagra-Mendoza, K., Rimolo-Donadio, R., 2020. Erosion quantification in runoff agriculture plots by multitemporal high-resolution UAS digital photogrammetry. IEEE J. Sel. Top. Appl. Earth Obs. Remote Sens 13, 6326–6336. https://doi.org/10.1109/JSTARS.2020.3027880.

Bagagiolo, G., Biddoccu, M., Rabino, D., Cavallo, E., 2018. Effects of rows arrangement, soil management, and rainfall characteristics on water and soil losses in Italian sloping vineyards. Environ. Res. 166, 690–704. https://doi.org/10.1016/j.envres.2018.06.048.

Barneveld, R.J., Seeger, M., Maalen-Johansen, I., 2013. Assessment of terrestrial laser scanning technology for obtaining high-resolution DEMs of soils. Earth Surf. Process. Landf. 38, 90–94. https://doi.org/10.1002/esp.3344.

Batey, T., 2009. Soil compaction and soil management - a review. Soil Use Manag. 25, 335–345. https://doi.org/10.1111/j.1475-2743.2009.00236.x.

Biddoccu, M., Ferraris, S., Opsi, F., Cavallo, E., 2016. Long-term monitoring of soil management effects on runoff and soil erosion in sloping vineyards in Alto Monferrato (North-West Italy). Soil Tillage Res. 155, 176–189. https://doi.org/10.1016/j.still.2015.07.005.

Biddoccu, M., Ferraris, S., Pitacco, A., Cavallo, E., 2017. Temporal variability of soil management effects on soil hydrological properties, runoff and erosion at the field

scale in a hillslope vineyard, North-West Italy. Soil Tillage Res. 165, 46–58. https://doi.org/10.1016/j.still.2016.07.017.
Blavet, D., De Noni, G., Le Bissonnais, Y., Leonard, M., Maillo, L., Laurent, J.Y., Asseline, J., Leprun, J.C., Arshad, M.A., Roose, E., 2009. Effect of land use and management on the early stages of soil water erosion in French Mediterranean vineyards. Soil Tillage Res. 106, 124–136. https://doi.org/10.1016/j.still.2009.04.010.
Boardman, J., Favis-Mortlock, D., 1998. Modelling soil erosion by water. In: Modelling Soil Erosion by Water. Springer, Berlin, Heidelberg, pp. 3–6. https://doi.org/10.1007/978-3-642-58913-3_1.
Bodhinayake, W., Si, B.C., Noborio, K., 2004. Determination of Hydraulic Properties in Sloping Landscapes from Tension and Double-Ring Infiltrometers. Vadose Zo. J. 3, 964–970. https://doi.org/10.2136/vzj2004.0964.
Borselli, L., Cassi, P., Torri, D., 2008. Prolegomena to sediment and flow connectivity in the landscape: a GIS and field numerical assessment. Catena 75, 268–277. https://doi.org/10.1016/j.catena.2008.07.006.
Buesa, I., Mirás-Avalos, J.M., De Paz, J.M., Visconti, F., Sanz, F., Yeves, A., Guerra, D., Intrigliolo, D.S., 2021. Soil management in semi-arid vineyards: combined effects of organic mulching and no-tillage under different water regimes. Eur. J. Agron. 123. https://doi.org/10.1016/j.eja.2020.126198.
Bunya, S., Dietrich, J.C., Westerink, J.J., Ebersole, B.A., Smith, J.M., Atkinson, J.H., Jensen, R., Resio, D.T., Luettich, R.A., Dawson, C., Cardone, V.J., Cox, A.T., Powell, M.D., Westerink, H.J., Roberts, H.J., 2010. A high-resolution coupled riverine flow, tide, wind, wind wave, and storm surge model for southern Louisiana and Mississippi. Part I: model development and validation. Mon. Weather Rev. 138, 345–377. https://doi.org/10.1175/2009MWR2906.1.
Cândido, B.M., Quinton, J.N., James, M.R., Silva, M.L.N., de Carvalho, T.S., de Lima, W., Beniaich, A., Eltner, A., 2020. High-resolution monitoring of diffuse (sheet or interrill) erosion using structure-from-motion. Geoderma 375, 114477. https://doi.org/10.1016/j.geoderma.2020.114477.
Capello, G., Biddoccu, M., Ferraris, S., Pitacco, A., Cavallo, E., 2017. Year-round variability of field-saturated hydraulic conductivity and runoff in tilled and grassed vineyards. Chem. Eng. Trans. 58, 739–744. https://doi.org/10.3303/CET1758124.
Carretta, L., Tarolli, P., Cardinali, A., Nasta, P., Romano, N., Masin, R., 2021. Evaluation of runoff and soil erosion under conventional tillage and no-till management: a case study in northeast Italy. Catena 197, 104972. https://doi.org/10.1016/j.catena.2020.104972.
Carrivick, J.L., Smith, M.W., Quincey, D.J., 2016. Structure from Motion in the Geosciences. John Wiley & Sons. https://doi.org/10.1002/9781118895818.
Cavalli, M., Trevisani, S., Comiti, F., Marchi, L., 2013. Geomorphometric assessment of spatial sediment connectivity in small Alpine catchments. Geomorphology 188, 31–41. https://doi.org/10.1016/j.geomorph.2012.05.007.
Chow, V.T., 1959. Open channel hydraulics. McGraw-Hill, New York.
Corti, G., Cavallo, E., Cocco, S., Biddoccu, M., Brecciaroli, G., Agnelli, A., 2011. Evaluation of Erosion Intensity and Some of Its Consequences in Vineyards from Two Hilly Environments Under a Mediterranean Type of Climate, Italy. Soil Eros. Issues Agric. https://doi.org/10.5772/25130.
Crema, S., Cavalli, M., 2018. SedInConnect: a stand-alone, free and open source tool for the assessment of sediment connectivity. Comput. Geosci. 111, 39–45. https://doi.org/10.1016/j.cageo.2017.10.009.
Cucchiaro, S., Cazorzi, F., Marchi, L., Crema, S., Beinat, A., Cavalli, M., 2019. Multi-temporal analysis of the role of check dams in a debris-flow channel: linking structural and functional connectivity. Geomorphology 345, 106844. https://doi.org/10.1016/j.geomorph.2019.106844.
Cucchiaro, S., Fallu, D., Zhang, H., Walsh, K., Oost, K., Brown, T., Tarolli, P., 2020. Multiplatform-SfM and TLS data fusion for monitoring agricultural terraces in complex topographic and landcover conditions. Remote Sens 12, 1946. https://doi.org/10.3390/rs12121946.
Di Giuseppe, A., Gambelli, A.M., Rossi, F., Nicolini, A., Ceccarelli, N., Palliotti, A., 2020. Insulating organic material as a protection system against late frost damages on the vine shoots. Sustain 12, 1–20. https://doi.org/10.3390/SU12156279.
Eisenbeiss, H., Sauerbier, M., 2011. Investigation of uav systems and flight modes for photogrammetric applications. Photogramm. Rec. 26, 400–421. https://doi.org/10.1111/j.1477-9730.2011.00657.x.
Eltner, A., Kaiser, A., Castillo, C., Rock, G., Neugirg, F., Abellán, A., 2016. Image-based surface reconstruction in geomorphometry-merits, limits and developments. Earth Surf. Dyn. 4, 359–389. https://doi.org/10.5194/esurf-4-359-2016.
Estornell, J., Ruiz, L.A., Velázquez-Martí, B., Hermosilla, T., 2011. Analysis of the factors affecting LiDAR DTM accuracy in a steep shrub area. Int. J. Digit. Earth 4, 521–538. https://doi.org/10.1080/17538947.2010.533201.
FAO, 2021. Soave Traditional Vineyards, Italy. ⟨http://www.fao.org/giahs/giahsaroundtheworld/designated-sites/europe-and-central-asia/soave-traditional-vineyards/en/⟩ (Accessed 2.2.21).
FAO, 2020. Soave Traditional Vineyards, Italy. ⟨http://www.fao.org/giahs/giahsaroundtheworld/designated-sites/europe-and-central-asia/soave-traditional-vineyards/en/⟩ (Accessed 2.2.21).
Fernandes, J., Bateira, C., Soares, L., Faria, A., Oliveira, A., Hermenegildo, C., Moura, R., Gonçalves, J., 2017. SIMWE model application on susceptibility analysis to bank gully erosion in Alto Douro Wine Region agricultural terraces. Catena 153, 39–49. https://doi.org/10.1016/j.catena.2017.01.034.
Ferrero, A., Usowicz, B., Lipiec, J., 2005. Effects of tractor traffic on spatial variability of soil strength and water content in grass covered and cultivated sloping vineyard. Soil Tillage Res. 84, 127–138. https://doi.org/10.1016/j.still.2004.10.003.
Flanagan, D.C., Nearing, M.A., 1995. USDA-water erosion prediction project: hillslope profile and watershed model documentation. Nserl Rep. 10, 1–123.
Gonçalves, G.R., Pérez, J.A., Duarte, J., 2018. Accuracy and effectiveness of low cost UASs and open source photogrammetric software for foredunes mapping. Int. J. Remote Sens. 39, 5059–5077. https://doi.org/10.1080/01431161.2018.1446568.
Greer, D.H., Weedon, M.M., 2012. Modelling photosynthetic responses to temperature of grapevine (Vitis vinifera cv. Semillon) leaves on vines grown in a hot climate. Plant, Cell Environ. 35, 1050–1064. https://doi.org/10.1111/j.1365-3040.2011.02471.x.
Heckmann, T., Cavalli, M., Cerdan, O., Foerster, S., Javaux, M., Lode, E., Smetanová, A., Vericat, D., Brardinoni, F., 2018. Indices of sediment connectivity: opportunities, challenges and limitations. Earth Sci. Rev. 187, 77–108. https://doi.org/10.1016/j.earscirev.2018.08.004.
Höhle, J., Höhle, M., 2009. Accuracy assessment of digital elevation models by means of robust statistical methods. ISPRS J. Photogramm. Remote Sens. 64, 398–406. https://doi.org/10.1016/j.isprsjprs.2009.02.003.
Jing, X., Chen, Y., Pan, C., Yin, T., Wang, W., Fan, X., 2019. Erosion failure of a soil slope by heavy rain: Laboratory investigation and modified GA model of soil slope failure. Int. J. Environ. Res. Public Health 16. https://doi.org/10.3390/ijerph16061075.
Jones, G.V., Hellman, E.W., 2003. Chapter 3: site assessment. In: Hellman, E. (Ed.), Oregon Viticulture, Fifth ed.,. Oregon State University Press, Corvallis, OR, pp. 44–50.
Julien, P.Y., Saghafian, B., Ogden, F.L., 1995. Raster-based hydrologic modeling of spatially-varied surface runoff. JAWRA J. Am. Water Resour. Assoc. 31, 523–536. https://doi.org/10.1111/j.1752-1688.1995.tb04039.x.
Ladefoged, T.N., McCoy, M.D., Asner, G.P., Kirch, P.V., Puleston, C.O., Chadwick, O.A., Vitousek, P.M., 2011. Agricultural potential and actualized development in Hawai'i: an airborne LiDAR survey of the leeward Kohala field system (Hawai'i Island). J. Archaeol. Sci. 38, 3605–3619. https://doi.org/10.1016/j.jas.2011.08.031.
Laflen, J.M., Lane, L.J., Foster, G.R., 1991. WEPP: a new generation of erosion prediction technology. J. Soil Water Conserv 46, 34–38.
Lai, J., Ren, L., 2007. Assessing the size dependency of measured hydraulic conductivity using double-ring infiltrometers and numerical simulation. Soil Sci. Soc. Am. J. 71, 1667–1675. https://doi.org/10.2136/sssaj2006.0227.
Lal, R., 2001. Soil degradation by erosion. L. Degrad. Dev. 12, 519–539. https://doi.org/10.1002/ldr.472.
Li, H., Gao, H., Zhou, Y., Xu, C.Y., Rengifo, M., Sælthun, N.R., 2020. Usage of SIMWE model to model urban overland flood: a case study in Oslo. Hydrol. Res 51, 366–380. https://doi.org/10.2166/nh.2020.068.
Lili, M., Bralts, V.F., Yinghua, P., Han, L., Tingwu, L., 2008. Methods for measuring soil infiltration: State of the art. Int. J. Agric. Biol. Eng. 1, 22–30. https://doi.org/10.3965/j.issn.1934-6344.2008.01.022-030.
Marques, M.J., García-Muñoz, S., Muñoz-Organero, G., Bienes, R., 2010. Soil conservation beneath grass cover in hillside vineyards under mediterranean climatic conditions (MADRID, SPAIN). L. Degrad. Dev. 21, 122–131. https://doi.org/10.1002/ldr.915.
Martínez-Casasnovas, J.A., Ramos, M.C., Ribes-Dasi, M., 2002. Soil erosion caused by extreme rainfall events: Mapping and quantification in agricultural plots from very detailed digital elevation models. Geoderma 105, 125–140. https://doi.org/10.1016/S0016-7061(01)00096-9.
Meinen, B.U., Robinson, D.T., 2020. Mapping erosion and deposition in an agricultural landscape: optimization of UAV image acquisition schemes for SfM-MVS. Remote Sens. Environ. 239, 111666 https://doi.org/10.1016/j.rse.2020.111666.
Mitas, L., Mitasova, H., 1998. Distributed soil erosion simulation for effective erosion prevention. Water Resour. Res. 34, 505–516. https://doi.org/10.1029/97WR03347.
Mitasova, H., Mitas, L., 2001. Multiscale soil erosion simulations for land use management. Landsc. Eros. Evol. Model. 321–347. https://doi.org/10.1007/978-1-4615-0575-4_11.
Mitasova, H., Thaxton, C., Hofierka, J., McLaughlin, R., Moore, A., Mitas, L., 2004. Path sampling method for modeling overland water flow, sediment transport, and short term terrain evolution in open source GIS. Dev. Water Sci. 55, 1479–1490. https://doi.org/10.1016/S0167-5648(04)80159-X.
Monteiro, A., Lopes, C.M., 2007. Influence of cover crop on water use and performance of vineyard in Mediterranean Portugal. Agric. Ecosyst. Environ. 121, 336–342. https://doi.org/10.1016/j.agee.2006.11.016.
Morin, J., Benyamini, Y., 1977. Rainfall infiltration into bare soils. Water Resour. Res. 13, 813–817. https://doi.org/10.1029/WR013i005p00813.
Morvan, X., Naisse, C., Malam Issa, O., Desprats, J.F., Combaud, A., Cerdan, O., 2014. Effect of ground-cover type on surface runoff and subsequent soil erosion in champagne vineyards in France. Soil Use Manag. 30, 372–381. https://doi.org/10.1111/sum.12129.
Myers, J.L., Wagger, M.G., 1996. Runoff and sediment loss from three tillage systems under simulated rainfall. Soil Tillage Res. 39, 115–129. https://doi.org/10.1016/S0167-1987(96)01041-0.
Nearing, M.A., Lane, L.J., Lopes, V.L., 1994. Modeling Soil Erosion. In: Soil Erosion Research Methods. Routledge.
Neteler, M., Mitasova, H., 2008. Open source GIS: A GRASS GIS approach, third edition. Int. Ser. Eng. Comput. Sci. https://doi.org/10.1007/978-0-387-68574-8.
Novara, A., Gristina, L., Saladino, S.S., Santoro, A., Cerdà, A., 2011. Soil erosion assessment on tillage and alternative soil managements in a Sicilian vineyard. Soil Tillage Res. 117, 140–147. https://doi.org/10.1016/j.still.2011.09.007.
Novara, A., Pisciotta, A., Minacapilli, M., Maltese, A., Capodici, F., Cerdà, A., Gristina, L., 2018. The impact of soil erosion on soil fertility and vine vigor. A multidisciplinary approach based on field, laboratory and remote sensing approaches. Sci. Total Environ. 622–623, 474–480. https://doi.org/10.1016/j.scitotenv.2017.11.272.
Novara, A., Stallone, G., Cerdà, A., Gristina, L., 2019. The effect of shallow tillage on soil erosion in a semi-arid vineyard. Agronomy 9. https://doi.org/10.3390/agronomy9050257.

Oz, I., Arav, R., Filin, S., Assouline, S., Furman, A., 2017. High-resolution measurement of topographic changes in agricultural soils. Vadose Zo. J. 16 https://doi.org/10.2136/vzj2017.07.0138.

Paiola, A., Assandri, G., Brambilla, M., Zottini, M., Pedrini, P., Nascimbene, J., 2020. Exploring the potential of vineyards for biodiversity conservation and delivery of biodiversity-mediated ecosystem services: a global-scale systematic review. Sci. Total Environ. 706, 135839 https://doi.org/10.1016/j.scitotenv.2019.135839.

Peyrard, X., Liger, L., Guillemain, C., Gouy, V., 2016. A trench study to assess transfer of pesticides in subsurface lateral flow for a soil with contrasting texture on a sloping vineyard in Beaujolais. Environ. Sci. Pollut. Res. 23, 14–22. https://doi.org/10.1007/s11356-015-4917-5.

Pijl, A., Barneveld, P., Mauri, L., Borsato, E., Grigolato, S., Tarolli, P., 2019. Impact of mechanisation on soil loss in terraced vineyard landscapes. Cuad. Investig. Geográfica 45. https://doi.org/10.18172/cig.3774.

Pijl, A., Quarella, E., Vogel, T.A., D'Agostino, V., Tarolli, P., 2021. Remote sensing vs. field-based monitoring of agricultural terrace degradation. Int. Soil Water Conserv. Res. 9, 1–10. https://doi.org/10.1016/j.iswcr.2020.09.001.

Pijl, A., Reuter, L.E.H., Quarella, E., Vogel, T.A., Tarolli, P., 2020. GIS-based soil erosion modelling under various steep-slope vineyard practices. Catena 193, 104604. https://doi.org/10.1016/j.catena.2020.104604.

Pijl, A., Wang, W., Straffelini, E., Tarolli, P., 2022. Soil and water conservation in terraced and non-terraced cultivations: an extensive comparison of 50 vineyards. Land Degrad. Dev. 33 (4), 596–610. https://doi.org/10.1002/ldr.4170.

Pineux, N., Lisein, J., Swerts, G., Bielders, C.L., Lejeune, P., Colinet, G., Degré, A., 2017. Can DEM time series produced by UAV be used to quantify diffuse erosion in an agricultural watershed? Geomorphology 280, 122–136. https://doi.org/10.1016/j.geomorph.2016.12.003.

Pirotti, F., Tarolli, P., 2010. Suitability of LiDAR point density and derived landform curvature maps for channel network extraction. Hydrol. Process. 24, 1187–1197. https://doi.org/10.1002/hyp.7582.

Poesen, J.W.A., Hooke, J.M., 1997. Erosion, flooding and channel management in Mediterranean environments of southern Europe. Prog. Phys. Geogr. Earth Environ. 21, 157–199. https://doi.org/10.1177/030913339702100201.

Prosdocimi, M., Burguet, M., Di Prima, S., Sofia, G., Terol, E., Rodrigo Comino, J., Cerdà, A., Tarolli, P., 2017. Rainfall simulation and structure-from-motion photogrammetry for the analysis of soil water erosion in Mediterranean vineyards. Sci. Total Environ. 574, 204–215. https://doi.org/10.1016/j.scitotenv.2016.09.036.

Remondino, F., Nocerino, E., Toschi, I., Menna, F., 2017. A critical review of automated photogrammetric processing of large datasets. Int. Arch. Photogramm Remote Sens. Spat. Inf. Sci. XLII-2/W5, 591–599. https://doi.org/10.5194/isprs-archives-XLII-2-W5-591-2017.

Renard, K.G., Foster, G.R., Weesies, G.A., Porter, J.P., 1991. RUSLE: revised universal soil loss equation. J. Soil Water Conserv. 46, 30–33.

Rodrigo-Comino, J., Lucas-Borja, M.E., Bertalan, L., Cerdà, A., 2020. Integrating in situ measurements of an index of connectivity to assess soil erosion processes in vineyards. Hydrol. Sci. J. 65, 671–679. https://doi.org/10.1080/02626667.2020.1711914.

Rodrigo Comino, J., Ruiz Sinoga, J.D., Senciales González, J.M., Guerra-Merchán, A., Seeger, M., Ries, J.B., 2016. High variability of soil erosion and hydrological processes in Mediterranean hillslope vineyards (Montes de Málaga, Spain). Catena 145, 274–284. https://doi.org/10.1016/j.catena.2016.06.012.

Ruiz-Colmenero, M., Bienes, R., Marques, M.J., 2011. Soil and water conservation dilemmas associated with the use of green cover in steep vineyards. Soil Tillage Res. 117, 211–223. https://doi.org/10.1016/j.still.2011.10.004.

Sanz-Ablanedo, E., Chandler, J.H., Rodríguez-Pérez, J.R., Ordóñez, C., 2018. Accuracy of unmanned aerial vehicle (UAV) and SfM photogrammetry survey as a function of the number and location of ground control points used. Remote Sens 10. https://doi.org/10.3390/rs10101606.

Smith, R.E., Goodrich, D.C., Woolhiser, D.A., Unkrich, C.L., 1995. KINEROS - a kinematic runoff and erosion model. In: Singh, V.P. (Ed.), Computer Models of Watershed Hydrology, pp. 697–732.

Szögi, A.A., Leib, B.G., Redulla, C.A., Stevens, R.G., Mathews, G.R., Strausz, D.A., 2007. Erosion control practices integrated with polyacrylamide for nutrient reduction in rill irrigation runoff. Agric. Water Manag. 91, 43–50. https://doi.org/10.1016/j.agwat.2007.04.003.

Tang, Q., Xu, Y., Bennett, S.J., Li, Y., 2015. Assessment of soil erosion using RUSLE and GIS: a case study of the Yangou watershed in the Loess Plateau, China. Environ. Earth Sci. 73, 1715–1724. https://doi.org/10.1007/s12665-014-3523-z.

Tarolli, P., Straffelini, E., 2020. Agriculture in hilly and mountainous landscapes: threats, monitoring and sustainable management. Geogr. Sustain. 1, 70–76. https://doi.org/10.1016/j.geosus.2020.03.003.

Townsend, C.G., 2011. Viticulture and the role of geomorphology: general principles and case studies. Geogr. Compass 5, 750–766. https://doi.org/10.1111/j.1749-8198.2011.00449.x.

Triplett, G.B., Dick, W.A., 2008. No-tillage crop production: a revolution in agriculture! agron. J 100, 153–165. https://doi.org/10.2134/agronj2007.0005c.

UNESCO, 2021. Le Colline del Prosecco di Conegliano e Valdobbiadene. ⟨https://whc.unesco.org/en/list/1571⟩ (Accessed 5.1.21).

Vergani, C., Graf, F., 2016. Soil permeability, aggregate stability and root growth: a pot experiment from a soil bioengineering perspective. Ecohydrology 9, 830–842. https://doi.org/10.1002/eco.1686.

Wang, W., Pijl, A., Tarolli, P., 2022. Future climate-zone shifts are threatening steep-slope agriculture. Nat. Food 3, 193–196. https://doi.org/10.1038/s43016-021-00454-y.